

A major purpose of the Technical Information Center is to provide the broadest dissemination possible of information contained in DOE's Research and Development Reports to business, industry, the academic community, and federal, state and local governments.

Although a small portion of this report is not reproducible, it is being made available to expedite the availability of information on the research discussed herein.

1

LA-UR--88-3948

DE89 003585

TITLE. RECENT HEAVY ION RESULTS FROM CERN AND BROOKHAVEN

AUTHOR(S) Barbara V. Jacak

SUBMITTED TO. LAMPF Workshop on Nuclear and Particle Physics on the
Light Cone, July 18-22, 1988, Los Alamos, NM.

DISCLAIMER

This report was prepared as an account of work sponsored by an agency of the United States Government. Neither the United States Government nor any agency thereof, nor any of their employees, makes any warranty, express or implied, or assumes any legal liability or responsibility for the accuracy, completeness, or usefulness of any information, apparatus, product, or process disclosed, or represents that its use would not infringe privately owned rights. Reference herein to any specific commercial product, process, or service by trade name, trademark, manufacturer, or otherwise does not necessarily constitute or imply its endorsement, recommendation, or favoring by the United States Government or any agency thereof. The views and opinions of authors expressed herein do not necessarily state or reflect those of the United States Government or any agency thereof.

By acceptance of this article the publisher recognizes that the U.S. Government retains a nonexclusive, royalty-free license to publish or reproduce the published form of this contribution or to allow others to do so, for U.S. Government purposes.

The Los Alamos National Laboratory requests that the publisher identify this article as work performed under the auspices of the U.S. Department of Energy.

MASTER

Los Alamos Los Alamos National Laboratory
Los Alamos, New Mexico 87545

RECENT HEAVY ION RESULTS FROM CERN AND BROOKHAVEN

BARBARA V. JACAK

Los Alamos National Laboratory

ABSTRACT

Results of the first round of ultrarelativistic heavy ion experiments at CERN and BROOKHAVEN are reviewed. The experiments measure global variables such as transverse energy and multiplicity to characterize the impact parameter of the collisions and compare with geometrical models of heavy ion collisions. Charged particle transverse momentum spectra are measured, and p-nucleus and nucleus-nucleus collisions look rather similar. The hardening of the spectrum at high p_t , previously observed in p-nucleus, is also present in heavy ion collisions. Two-particle interferometry has been used to study the pion source in central collisions. For analysis of all pion pairs, this looks approximately like the tube cut through the target by the projectile, but mid-rapidity pion pairs indicate a large, nearly spherical, very chaotic source. Study of dimuon production in the J/ψ mass region has shown a suppression of J/ψ with respect to the continuum in central compared to peripheral collisions. This could be a signal of deconfinement, but careful studies are underway to determine the magnitude of such an effect from nuclear absorption.

INTRODUCTION

The availability of ultrarelativistic heavy ion beams at CERN and Brookhaven allows investigation of the physical properties of a state of high energy density in nuclear matter. The interest is driven by the expectation that a new state of matter, in which quarks and gluons are deconfined, is produced when the density is large compared to the density inside hadrons. This prospect is supported by QCD calculations,¹ which predict a phase transition at temperatures of ≈ 200 MeV. Heavy ion collisions at ultrarelativistic energies are predicted to provide the energy densities required for deconfinement (greater than $\approx 2 - 3$ GeV/fm³).

The use of heavy projectile and target nuclei should allow characterization of the high temperature, high density region by increasing its volume. This is a difficult task as the system is very short lived and rather small, extending over only several fm. It then expands and hadronizes; experimental observations are made much later, on a time scale of 10^{13} fm. Clearly, the interesting physical processes are hidden behind expansion of the system, reconfinement and hadronization. The search for evidence of a new phase of matter is further complicated by the coexistence of the two phases, which may still be very important at these energies.

Among the goals of the first experiments are investigation of the energy density and spatial extent of the highly excited central rapidity region to address whether the necessary conditions for deconfinement have been satisfied. This requires an understanding of the reaction dynamics, including geometry effects, the extent of nuclear transparency and a study of the independence of nucleon-nucleon collisions within the large projectile and target nuclei. Once it is possible to classify the events, according to impact parameter for example, there are a number of experimentally accessible probes for the initial state.

The first particles emitted as the reaction progresses are the direct photons and lepton pairs. These do not interact much with the surrounding cold matter, and emerge relatively undisturbed. The spectra of these particles can provide information about the temperature of the system early in the reaction.² The system subsequently expands and hadrons are emitted. The transverse momentum spectra of the hadrons allow study of the expansion phase of the collisions. Comparison of the $\langle p_t \rangle$ for species of different masses, such as π , K, \bar{p} , may provide evidence of hydrodynamic expansion of the hot central region.³

Study of J/ψ production can be very informative as the J/ψ 's are formed very early in the collision, and must propagate through the hot, dense

region. During this time, color screening keeps $c\bar{c}$ pairs apart if the quarks are deconfined, preventing formation of J/ψ .⁴ As J/ψ 's are not created during the hadronization process, the final population is not much different from that at early times. Interpretation of the J/ψ results, however, requires a thorough understanding of the interaction of J/ψ 's with dense hadronic matter, as they must pass through the central region of the collision even if there is no phase transition, and also through a fraction of the target remnant.

The strangeness content of particles produced in heavy ion collisions has been suggested as a possible signal for quark-gluon plasma.⁵ A plasma in chemical equilibrium will contain equal amounts of $u\bar{u}$, $d\bar{d}$ and $s\bar{s}$ pairs. During the transition back to hadronic matter, this ratio is changed by gluon decay, but an excess of strange quarks should be left.

All of these probes can be influenced by the dynamical evolution of the reaction. Because of this, the survey experiments must also register global quantities to describe the reaction. These include analysis of the shape of the energy flow through $\approx 4\pi$ measurement of the charged particle multiplicity and/or transverse energy, and careful study of the fluctuations in the multiplicity and energy flow. In addition, particle interferometry may be used to make a "snapshot" of the system at the time of particle emission.⁶

THE EXPERIMENTS

Here we will discuss results from four experiments performed with 200 and 60 GeV/A oxygen and sulfur beams at CERN and from two experiments at Brookhaven with 10 and 14.5 GeV/A silicon beams. The HELIOS experiment at CERN combines 4π calorimetric coverage with measurement of charged particle multiplicity, inclusive particle spectra, lepton pairs and photons. WA80 includes a highly segmented photon detector and identification of target rapidity particles, with a measurement of multiplicity and mid to forward rapidity calorimetry. NA35 consists of a streamer chamber,

allowing reconstruction of a large fraction of the particles, accompanied by mid-range and forward calorimetry. NA38 is a dimuon spectrometer optimized to study high mass pairs (J/ψ), with event characterization by means of E_t (neutral). At Brookhaven, experiment E802 features a magnetic spectrometer with excellent particle identification capabilities, along with measurements of multiplicity, E_t in the forward direction and the energy carried by neutral particles, E_{tot}^0 , which is proportional to E_t . E814 has 4π calorimetry with tracking of particles at very forward angles.

TRANSVERSE ENERGY AND MULTIPLICITY DISTRIBUTIONS

Figure 1 shows charged particle multiplicity distributions measured by WA80 for 60 and 200 GeV/A oxygen on various targets.⁷ The data were measured over the rapidity range $-1.7 < \eta < 4.2$, and include midrapidity. The transverse energy distributions for the same beams on W, Ag and Al targets in the HELIOS experiment⁸ are presented in Figure 2. The main feature of both distributions is a long plateau followed by a steeply falling tail, reflecting the shape of the overlap integral of nuclear densities in collisions with random impact parameters.⁹

The large value of E_t attained in these collisions is quite striking. For 200 GeV/A projectiles, E_t values up to 200 GeV are reached in the rapidity region $-0.1 < \eta < 2.9$; adding the E_t for $\eta > 2.9$ increases this to 280 GeV. This is approximately 0.7 of the kinematic limit, and shows that nuclei are not transparent to one another at these beam energies. An important first result is that the energy density is still increasing at 200 GeV/A beam energy.

The curves in Fig. 2 are fits to the geometrical overlap integral, folded with a Gaussian distribution in E_t for each N-N collision.⁹ This procedure yields an excellent description of the data, with a fitted mean of approximately 1 GeV, which may be compared with the mean E_t of ≈ 1.4 GeV

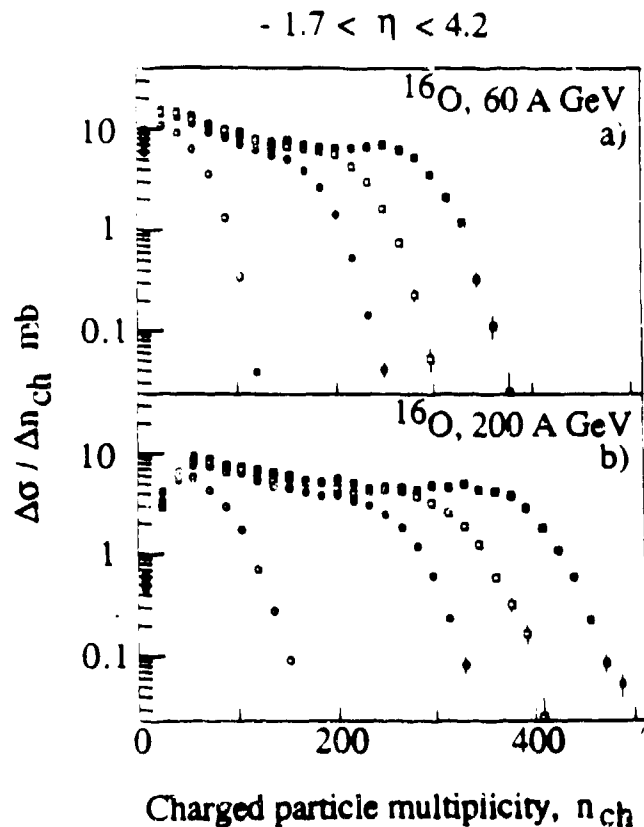


Fig. 1. The charged particle multiplicity distributions measured by WA80 for O + Au at a) 60 GeV/A and b) 200 GeV/A.

in p-p collisions at $\sqrt{s} = 20$ GeV. The widths of the fitted E_t distributions, however, are considerably larger than those observed in p-p collisions. Analysis of fluctuations in the transverse energy is underway to search for deviations from superposition of independent nucleon-nucleon collisions.¹⁰

From the geometrical picture, it is clear that the large values of E_t arise from the more central collisions. One would then expect the collisions with large E_t to show little energy going forward. This is indeed the case, as has been shown by WA80. They find a strong anticorrelation between transverse energy observed at midrapidity and energy observed in their forward calorimeter. Consequently experiments may choose among several methods

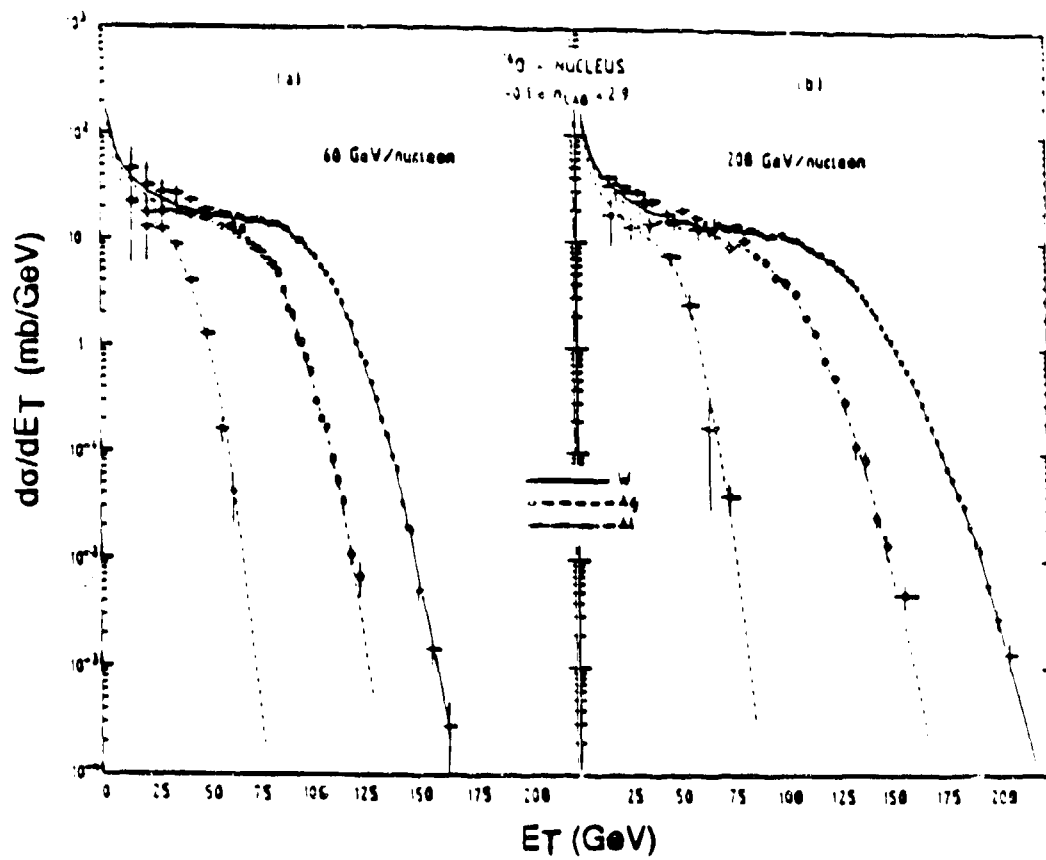


Fig. 2. The transverse energy distributions measured by HELIOS for O + W, Ag, Al at a) 60 GeV/A, b) 200 GeV/A. The curves are fits to the geometrical overlap integral, folded with a Gaussian distribution in E_t for each N-N collision.²

of identifying central collisions: large observed transverse energy, large observed multiplicity, or lack of forward energy.

Figure 3 shows results from Brookhaven. Figure 3A is from E814, showing the transverse energy produced by 10 GeV/A silicon beams on Al, Cu and Pb targets,¹¹ and Fig. 3B shows the distribution of the total energy carried by neutral particles measured in the angular range of 10 to 32 degrees in the laboratory by E802.¹² Note that the tails of the distributions from the heavier targets lie on top of one another. This shows that targets heavier than copper look very similar to projectiles at these energies, suggesting that

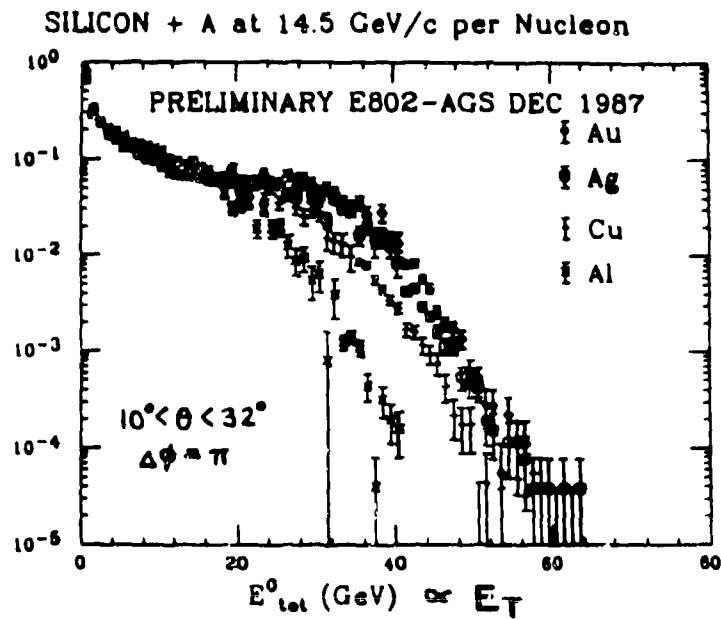
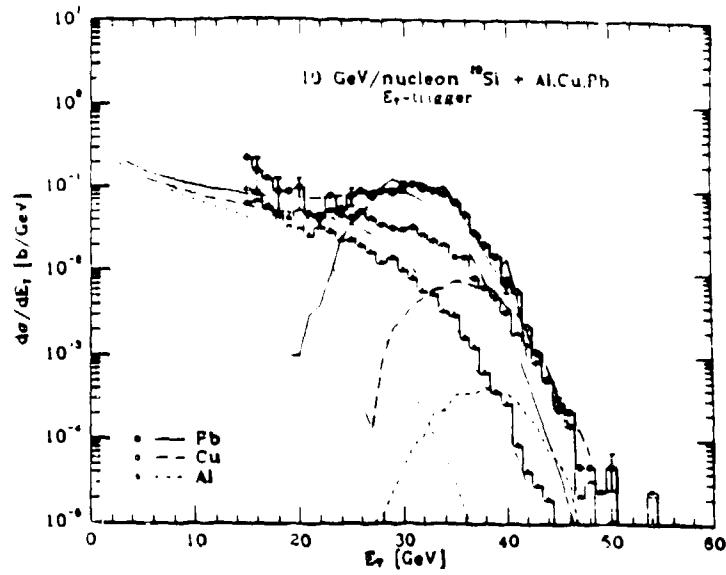


Fig. 3. Transverse energy distributions at Brookhaven. a) E_T measured by E814 for 10 GeV/A Si + various targets. b) $E_{T, \text{tot}}^0$, which is proportional to E_T , measured by E802 for 14.5 GeV/A Si + various targets.

the projectile does not penetrate the entire target nucleus. The measured distributions in both experiments are consistent with full stopping. E814

finds agreement of the measured E_t distributions with predictions from a fireball model assuming full stopping. E802 finds that their distributions of transverse energy carried by neutral particles can be well described by a superposition of proton-nucleus collisions.

The energy densities may be estimated from the measured E_t distributions. At Brookhaven, in the stopping regime, one can calculate the energy density in the fireball formed to be about $1 \text{ GeV}/\text{fm}^3$. In the non-stopping regime at CERN, the job is a bit more difficult. Estimates using the fraction of energy left in the fireball and using the Bjorken model¹³ which assumes free streaming of the projectile and target through one another both yield values in the region $1\text{-}3 \text{ GeV}/\text{fm}^3$.

One of the most important questions addressed by the first experiments concerns the makeup of the energy flow. We would like to determine whether the energy is carried by particles in the same way as in p-p collisions, or if the particle types, rapidities or spectra are modified by collective effects and/or a phase transition. This question is addressed by measurement of both transverse energy and multiplicity for each event. Figure 4 shows the multiplicity and transverse energy plotted against one another, Fig. 4A is from E802 at $14.5 \text{ GeV}/A$ and Fig. 4B is from WA80 at $200 \text{ GeV}/A$. It is clear that the relationship between the two quantities is linear at both energies, and also holds for the most central collisions. Therefore we conclude that the large transverse energies arise via formation of many charged particles rather than by a large change in the momentum distribution of produced particles. From the HELIOS multiplicity measurements together with the known calorimeter response (55% of the observed E_t arises from charged particles), we may estimate an average p_t per particle of $\approx 340 \text{ MeV}/c$.

Figure 5 shows the pseudorapidity distributions of both E_t and charged particle multiplicity measured by HELIOS for central collisions of $200 \text{ GeV}/A$ O + W. Though the comparison is limited by the calorimeter granularity,

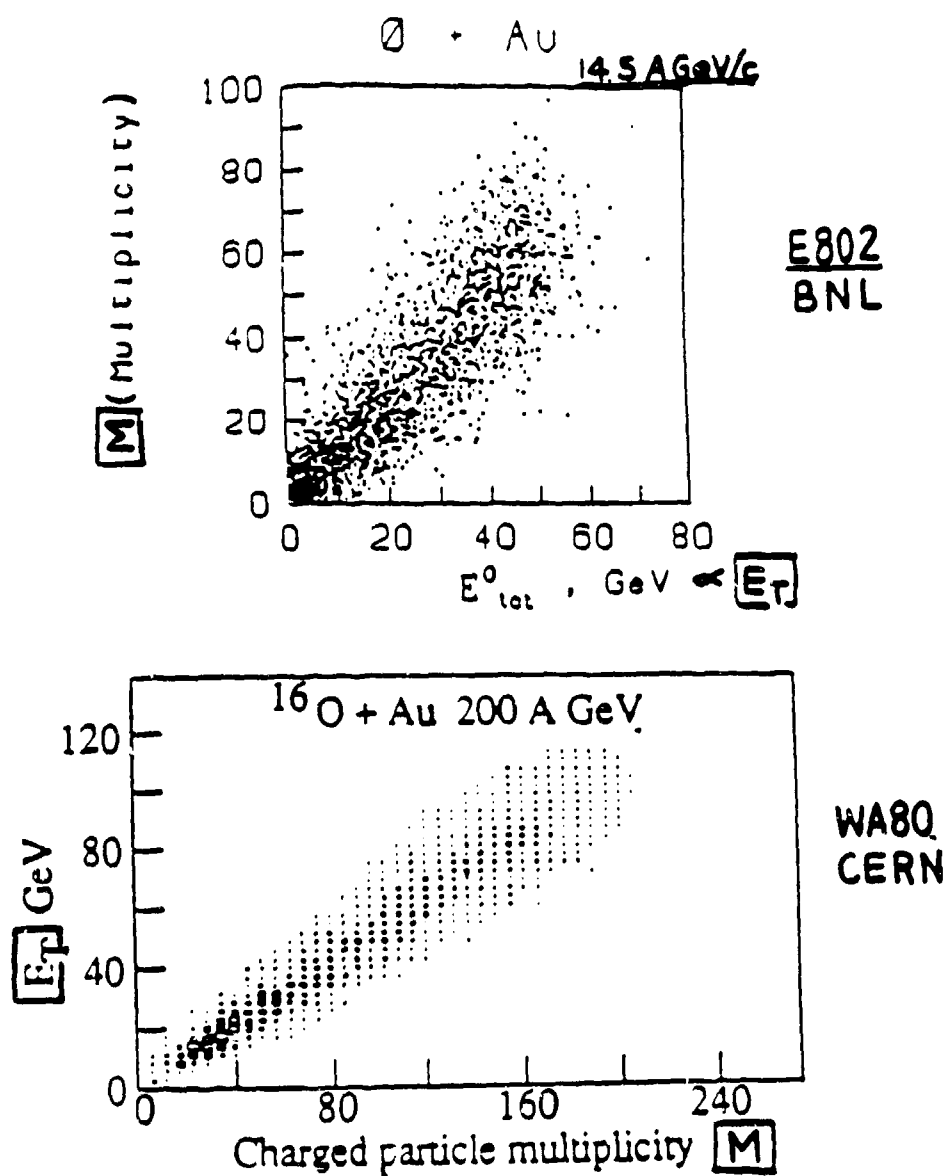


Fig. 4. Multiplicity vs. transverse energy for a) 14.5 GeV/A O + Au from E802 b) 200 GeV/A O + Au from WA80.

the two distributions agree rather well. They show a broad peak with maximum density between $\eta = 2$ and 2.5, clearly shifted backward from the p-p center of mass, $\eta \approx 3$. The values are close to $\eta = 2.4$, the center of mass rapidity characteristic of a system of 16 projectile nucleons stopped by 50 nucleons from the target. It should be noted that the shift of the peak

to smaller rapidity is impact parameter dependent. All the experiments as well as emulsion studies show that this shift is largest for the most central collisions. Also shown are $dE_t/d\eta$ predictions from IRIS¹⁴, an event generator incorporating nucleus-nucleus collision geometry with the dual parton model.¹⁵ The calculation is clearly more forward peaked than the data, and the rapidity densities in the backward region are underpredicted. A shift of particles to smaller rapidities could be expected from cascading of produced particles in the target spectator matter.

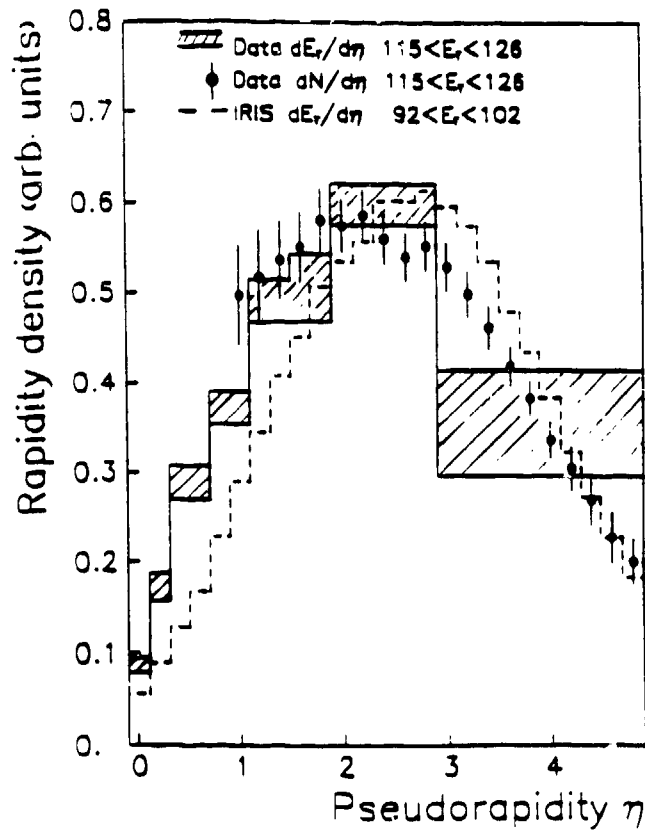


Fig. 5. Comparison of HELIOS pseudorapidity distributions of transverse energy (solid lines), charged particle multiplicity (points), and IRIS prediction of $dE_t/d\eta$ (dotted line).

HADRON MOMENTUM SPECTRA

From the E_t and multiplicity measurements we have learned that there are no drastic changes in the nature of the charged particles emitted; larger E_t is the result of more charged particles. Nevertheless, a direct measurement is necessary to study the details of the charged particle momentum spectra. These may indicate the degree of thermalization reached in the collision. Deviations from an exponential spectrum may provide evidence for a boost in p_t , showing that the particles gain a radial flow velocity from collective expansion of the central region. It has also been suggested that the formation and decay of a plasma will stiffen the hadron p_t spectra,¹⁸ so we need to compare the spectra produced in heavy ion reactions with those from p-p collisions. To aid in understanding the charged particle spectra, the transverse energy flow can be used to sort events according to impact parameter and energy deposition.

HELIOS measures charged particles with a magnetic spectrometer which views the target through a narrow slit in the calorimeter wall, covering the pseudo-rapidity interval $0.9 < \eta < 1.9$. Figure 6 shows the transverse momentum spectra for negative particles in the spectrometer in p + W, O + W and S + W collisions at 200 GeV/A. The dashed lines are the result of a parameterization combining FNAL and CERN ISR^{17,18} measurements of charged particles, taking into account the c.m. energy dependence, the rapidity, and the well-known hardening of the p_t spectra in p-A collisions.^{18,19}

All three data sets are well described by the parameterization, indicating that charged particles emitted in nucleus-nucleus collisions are very similar to those from proton-nucleus collisions. The p_t spectra clearly cannot be described by a single exponential, and HELIOS has derived the inverse slopes in the regions $0.5 < p_t < 2.0$ GeV/c and $0.1 < p_t < 0.2$ GeV/c. The results are ≈ 190 MeV/c and 85 MeV/c, respectively. The rise in cross section at low p_t has also been observed in p-nucleus collisions at Fermilab.¹⁹

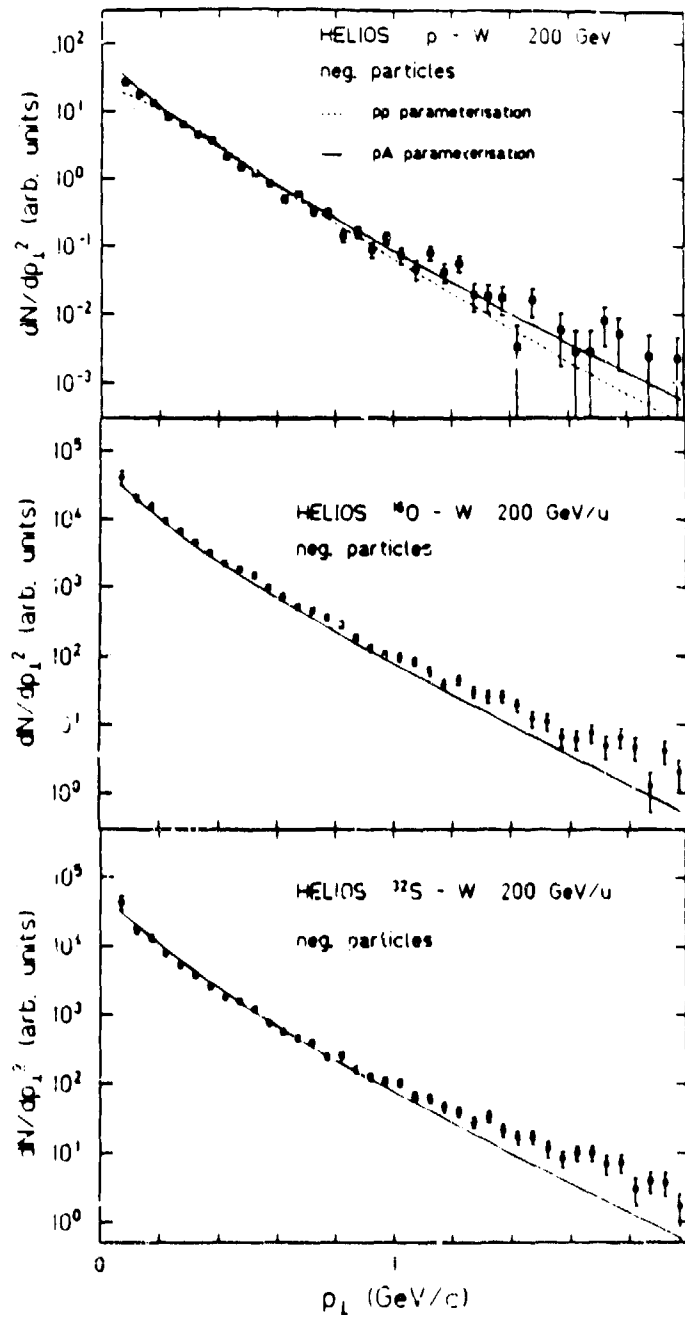


Fig. 6. p_t spectra of negative particles detected in the HELIOS external spectrometer for a) p + W, b) O + W, c) S + W at 200 GeV/A. The dashed line shows the results of a parameterization of p-p and p-A data described in the text.

and reported by NA35²⁰ for particles at $2 < y < 3$. The effect appears to be somewhat smaller for the higher rapidities, consistent with expectations for a target fragmentation effect. At high p_t the spectra show an excess; this effect was already observed in p-nucleus collisions^{21,18} some years ago and is referred to as the Cronin effect. The Cronin effect was found to scale with the target size. It has been suggested that the effect arises from parton multiple scattering, in which case it should be present in nucleus-nucleus collisions at least as strongly as in p-nucleus collisions.

Dividing the sulfur and oxygen spectra by one another, the ratio is not significantly different from one, over the entire p_t spectrum. This indicates little difference between oxygen and sulfur projectiles on a heavy target. The sulfur-proton and oxygen-proton ratios, however, rise slightly above one for $p_t > 1.3$ GeV/c. WA80 has fitted slopes to the π^0 spectra for $0.8 < p_t < 2.0$ GeV/c from p and O + Au targets. They find a slight rise in the slope for oxygen relative to proton beams. This difference between proton and heavy ion projectiles may arise due to a larger contribution of parton multiple scattering in the case of heavy projectiles.

To study the impact parameter dependence of the p_t spectra, WA80 has used the energy measured in the forward calorimeter to break up the O + Au data set into peripheral and central collisions. Figure 7 shows the π^0 transverse momentum spectra for the two data sets and also the slopes fit to the region $0.8 < p_t < 2.0$ GeV/c. Central collisions are defined as those with 30% or less of the beam energy found in the forward calorimeter. The spectra are somewhat different in shape, and the slope for central collisions is 30 MeV/c larger than for peripheral collisions. HELIOS has investigated the features of the spectra for central collisions to see whether the events in the tails of the distributions show any changes in the p_t spectra. Figure 8 presents ratios of the negative particle p_t spectra for events in different regions of E_t , to allow careful comparison of the spectral shape over the

200 A GeV O + Au
ZDC-dependence

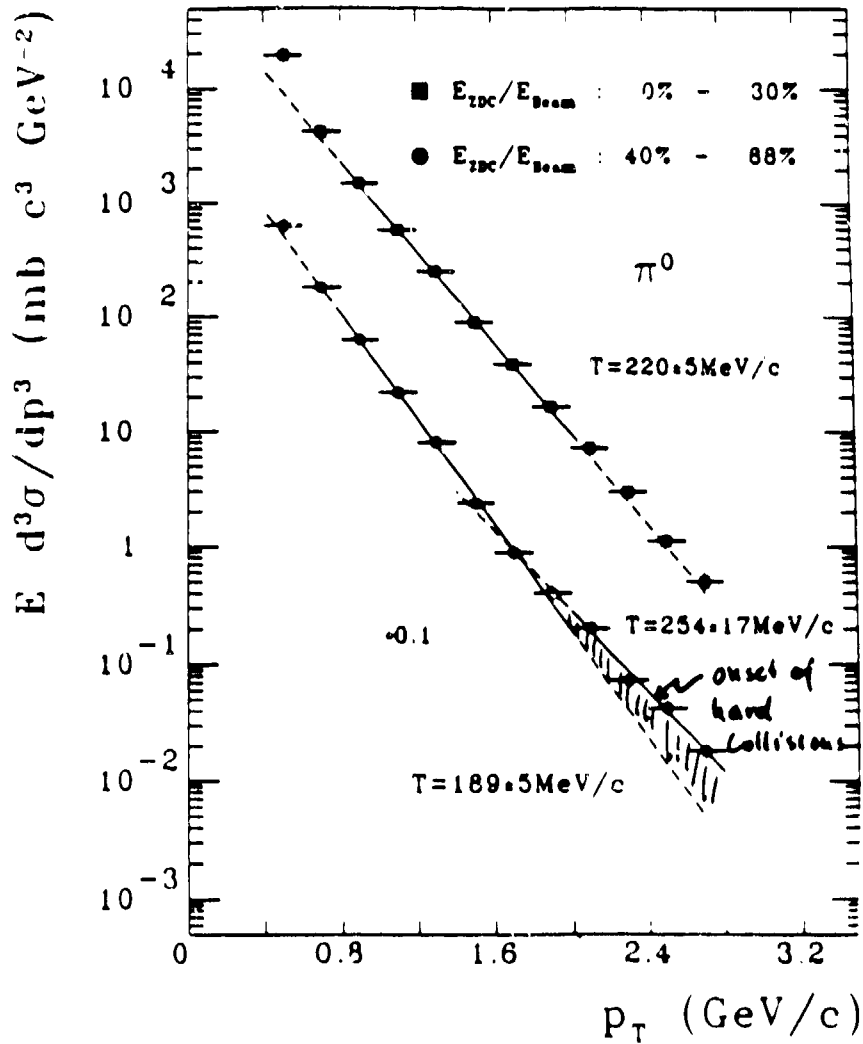


Fig. 7. p_t spectra of π^0 measured by WA80 for 200 GeV/A O + Au. The data are separated into central (upper curve) and peripheral (lower curve) collisions.

entire p_t range. The ratios shown are normalized by the number of events in each spectrum. The reference spectrum is taken from events with $55 < E_t < 100$ GeV, which lie in the plateau of the E_t distribution and correspond to

near overlap of the projectile and target. The events analyzed have $E_t > 100$ MeV, and represent only about 10% of the total cross section, i.e. the most central collisions. All four curves are flat within statistical errors, and should be relatively insensitive to systematic errors. They indicate that the transverse momentum spectrum of charged particles does not change with impact parameter once good overlap of projectile and target has been reached. This is an important result as it indicates that there is no hardening of the spectra when one chooses the most violent collisions producing very large transverse energies.

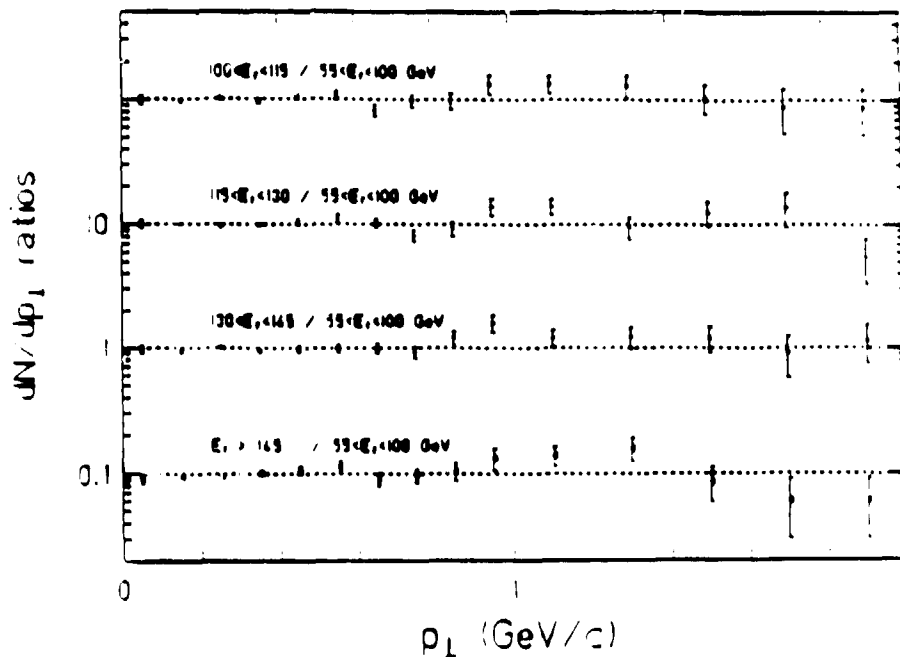


Fig. 8. Ratios of HELIOS negative particle spectra from O + W collisions at 200 GeV/A, plotted as a function of p_t . The ratios are normalized by the number of events in each spectrum. The four curves correspond to four regions of E_t , all normalized to the negative particle spectrum in events with $55 \text{ GeV} < E_t < 100 \text{ GeV}$. The curves are offset by factors of 10 for clarity.

To study the charged particle spectra over the entire range of impact parameters, HELIOS calculates the mean p_t of the distribution over the limited range $0.4 < p_t < 2.0$ GeV/c. The values are then extrapolated to the

mean of the entire spectrum under the assumption of a purely exponential shape. This method yields $\langle p_t \rangle$ which is not sensitive to the low p_t rise; the resulting values should be free of target effects and may be compared with p-p collisions. The $\langle p_t \rangle$ thus obtained can still, however, be affected if the spectral shape is not exponential. We have seen, for example, from Figures 6 and 7 that the spectra show a second component for $p_t \geq 1.5 \text{ GeV}/c$, where one might expect to see effects of multiple hard scattering processes.¹⁸ $\langle p_t \rangle$ vs. E_t for negative particles from 200 GeV/A S + W is plotted in Figure 9.

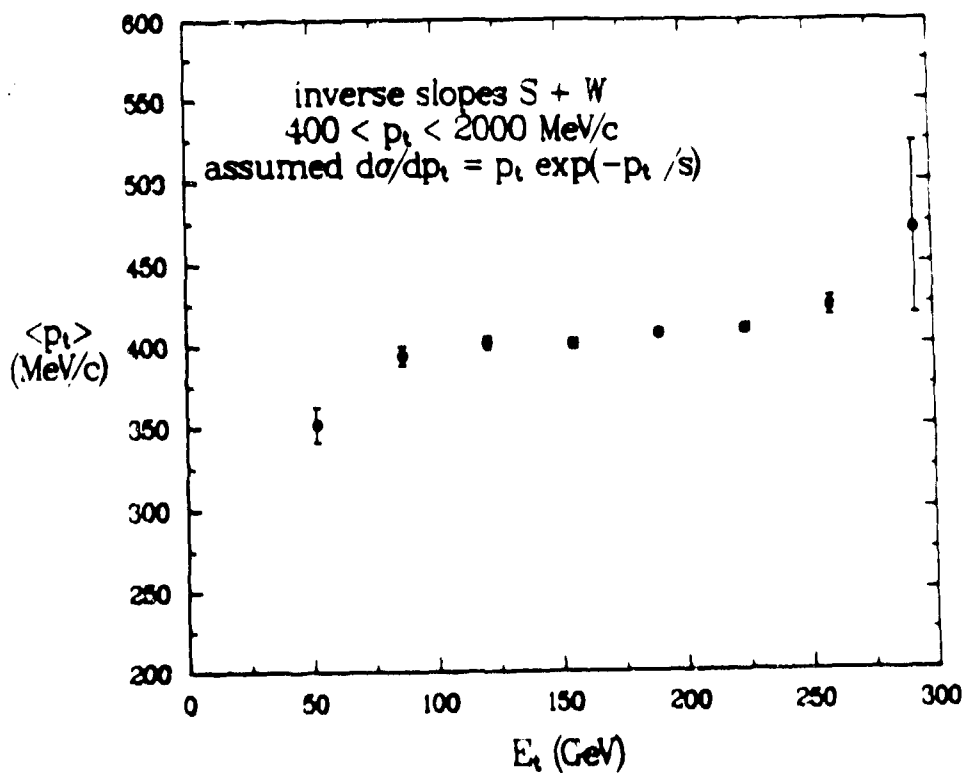


Fig. 9. $\langle p_t \rangle$ as a function of E_t for 200 GeV/A S + W. The $\langle p_t \rangle$ is derived from the measured spectra by correcting the mean value in the range $0.4 < p_t < 2.0 \text{ GeV}/c$ under the assumption of an exponential spectrum.

Central collisions, with $E_t \geq 80 \text{ GeV}$, yield a constant $\langle p_t \rangle$ of $400 \text{ MeV}/c$. This should be compared with the IRIS prediction of $300 \text{ MeV}/c$ for pions

in the HELIOS spectrometer acceptance.¹⁴ For $E_t \leq 60$ GeV, corresponding to relatively peripheral collisions, $\langle p_t \rangle$ is lower, falling by ≈ 50 MeV/c for the events with the lowest E_t . This is the same magnitude as the effect seen by WA80. It is important to remember that the Cronin effect will cause an increase in $\langle p_t \rangle$ of about 30 MeV/c, and may be important in the comparison of peripheral and central collisions (and is certainly important in the comparison of the heavy ion values with p-p collisions). An increase in $\langle p_t \rangle$ with multiplicity or E_t of the collisions, similar to what is observed, is predicted in models incorporating a hydrodynamical expansion of the highly excited central region.³ However, the p_t spectrum should also be strongly influenced by the hadronization process, making interpretation of the observed change more difficult.

PION INTERFEROMETRY

Experiment NA35 at CERN has taken advantage of its unique ability to reconstruct a large fraction of the particle momenta in each event. In addition to analyzing multiplicity and transverse momentum distributions they have studied correlations among particles. Such correlation measurements can yield space-time information about the interaction region.⁵ As pions are bosons, the probability of observing two or more simultaneously is enhanced for pions in the same or nearly the same state by the symmetry requirement of their wavefunctions. The enhancement can be used to describe the pion source by folding a particular model for the space-time geometry and dynamics of the source into the symmetrization requirement. This is then compared with the experimental correlation function.

NA35 has taken 105 central O + Au collisions at 200 GeV/A, with an average π^- multiplicity of ≈ 86 , and formed all unique pion pair combinations per event to make the correlation function. The background is formed by taking pairs of pions from different events. The static Gaussian distribution model,²² where the pion source points are assumed to be gaussian in both space and time, is used to fit the experimental correlation function and extract pion source parameters. A correlation function is constructed from the data, as a function of Q_T and Q_L , the momentum difference between the two pions in the transverse and longitudinal direction. This is then compared with the function from the Gaussian model

mean of the entire spectrum under the assumption of a purely exponential shape. This method yields $\langle p_t \rangle$ which is not sensitive to the low p_t rise; the resulting values should be free of target effects and may be compared with p-p collisions. The $\langle p_t \rangle$ thus obtained can still, however, be affected if the spectral shape is not exponential. We have seen, for example, from Figures 6 and 7 that the spectra show a second component for $p_t \geq 1.5 \text{ GeV}/c$, where one might expect to see effects of multiple hard scattering processes.¹⁸ $\langle p_t \rangle$ vs. E_t for negative particles from 200 GeV/A S + W is plotted in Figure 9.

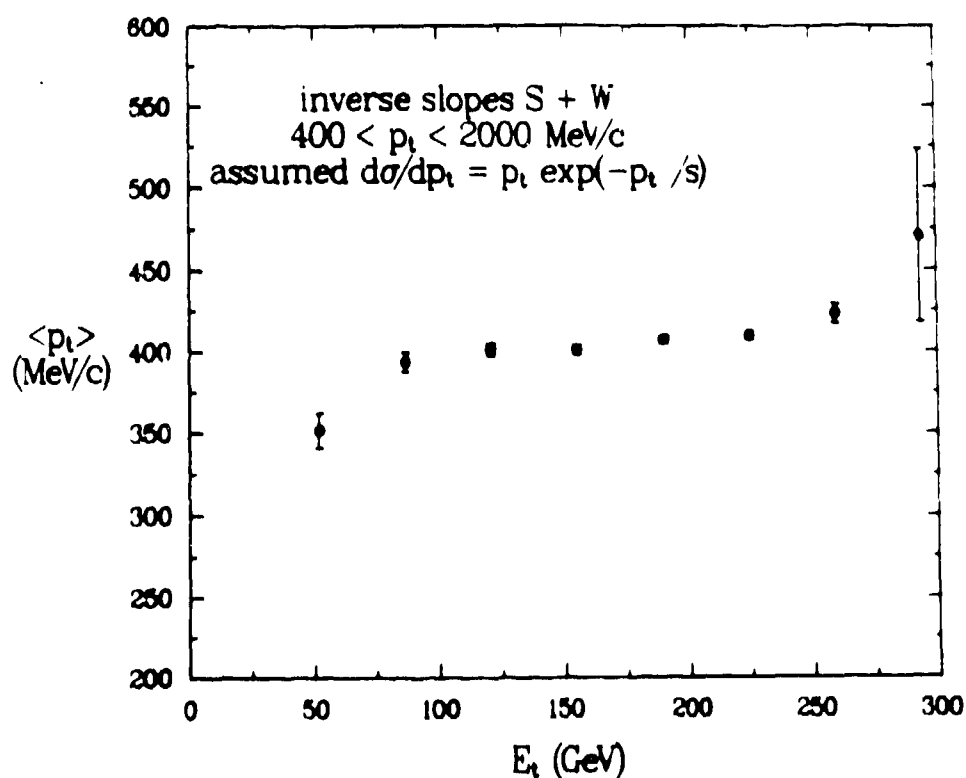


Fig. 9. $\langle p_t \rangle$ as a function of E_t for 200 GeV/A S + W. The $\langle p_t \rangle$ is derived from the measured spectra by correcting the mean value in the range $0.4 < p_t < 2.0 \text{ GeV}/c$ under the assumption of an exponential spectrum.

Central collisions, with $E_t \geq 80 \text{ GeV}$, yield a constant $\langle p_t \rangle$ of 400 MeV/c. This should be compared with the IRIS prediction of 300 MeV/c for pions

$$C(Q_T, Q_L) = A[1 + \lambda \exp(-Q_T^2 R_T^2/2 - Q_L^2 R_L^2/2)]$$

where R_T and R_L are the transverse and longitudinal radii of the source with respect to the beam axis, and λ is the chaoticity parameter (in this model $\lambda = 1$ implies totally chaotic pion emission, $\lambda = 0$ implies totally coherent emission). The source lifetime dependence is omitted as the data are not sensitive to it. The parameters R_T , R_L , and λ are varied until the calculated correlation function fits the measured one.

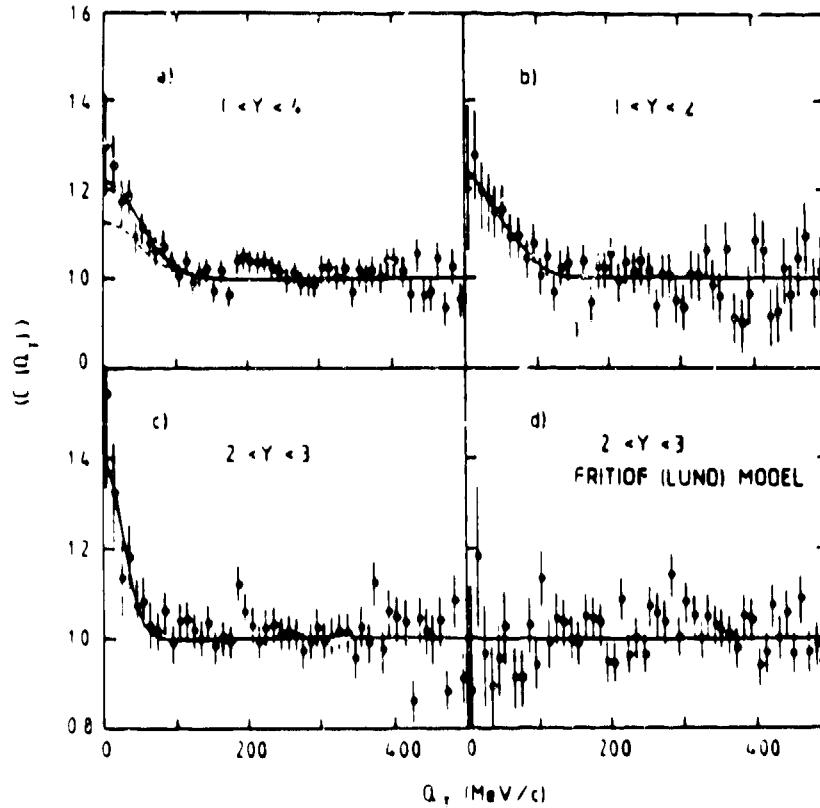


Fig. 10. Correlation functions for pion pairs detected in 3 rapidity regions by NA35 (a-c). d) shows the correlation function of pion pairs from the FRITIOF¹⁹ event generator, which does not contain Bose-Einstein statistics.

Figure 10 shows the correlation functions for pion pairs²³ in three rapidity regions: a large acceptance ($1 < y < 4$), target ($y < 2$), and central ($2 < y < 3$), along with the correlation function for pions from the LUND model for heavy ions²⁴ which does not contain Bose-Einstein statistics. Fits

with the Gaussian model are also shown; the resulting parameters are plotted in Fig. 11 for data from the full rapidity region and from central rapidity. The contours give the maximum likelihood values for 1σ (solid line) and 2σ (dashed line). The full rapidity data yield $R_t \approx 4$ fm, $R_L \approx 3$ fm and $\lambda \approx 0.3$. The value for R_T is comparable to that of the oxygen projectile and suggests that very little transverse expansion has occurred before pion freezeout. If R_L is expressed as a time, the fitted value is similar to the traversal time of the projectile through the target. A small value of λ indicates coherent emission of the pions. So the picture from the large rapidity region is of pion emission rather early in the collision with little time for expansion and thermalization. For the central rapidity region the values of R_T and R_L are much larger, and λ close to 1 indicates a very chaotic, perhaps thermalized source. This says that the central region expands to a large, nearly spherical thermalized object, encouraging the search for signals of a phase transition.

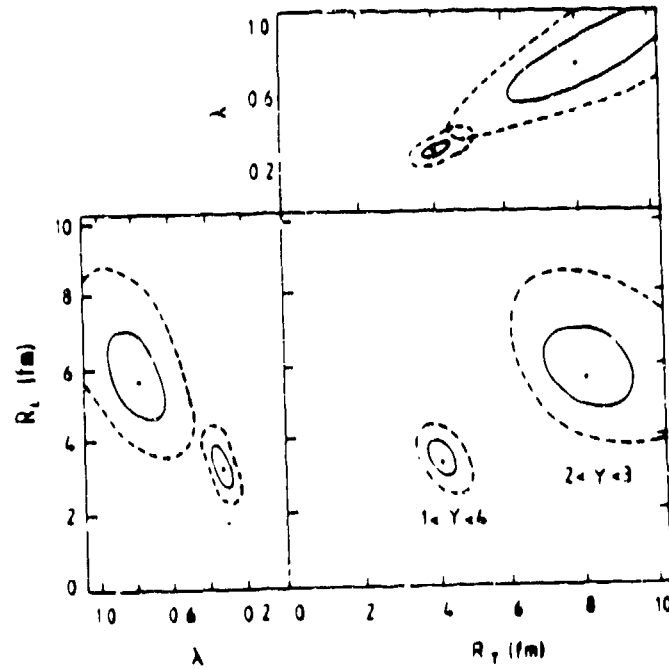


Fig. 11. Maximum likelihood contours for Gaussian fits to pion pairs in two rapidity intervals, projected onto 3 planes in (R_T, R_L, λ) parameter space. The solid line is the 1σ contour and the dashed line 2σ .

STRANGENESS PRODUCTION

In order to investigate the strangeness content of the particles produced at Brookhaven energies, E802 has built a spectrometer with drift chambers for the momentum measurement and plastic scintillators with time resolution of ≈ 75 psec for time-of-flight measurement.²⁵ Figure 12 shows the particle identification capabilities of this device. Using this system they have measured the K/π ratios for Si + Au collisions at 14.5 GeV/A, searching for ratios significantly greater than those observed in p-p collisions ($K^+/\pi^+ = 5-10\%$ and $K^-/\pi^- = 1-5\%$, depending on the angle and p_t). They find $K^+/\pi^+ = 19 \pm 5\%$ for peripheral collisions and $25 \pm 5\%$ for central collisions. K^-/π^- ratios are not very different from values observed in p-p collisions. The K^+/π^+ ratios observed in the heavy ion collisions are considerably higher than for p-p; the p_t dependence has been studied and the ion ratios are consistently higher than those for p-p and p-nucleus collisions. This has caused great interest as an enhancement of strange particles has been predicted as a signal of deconfinement.⁵ However, it still remains to be determined whether this effect is due to K^+ enhancement or π^+ suppression. Clearly, the pions must be formed in a dense, baryon-rich region (we have seen that the nuclei stop each rather well at these energies) and must also traverse some target spectator matter. Therefore the measured K/π ratios may be greatly affected by nuclear absorption effects on the π .

LEPTON PAIR DATA

Leptons are produced early in the collision, and can yield information about conditions at early times. Also, leptons are interesting because, unlike hadrons, their spectra are not modified by the hadronization process.

Dimuon results from NA38²⁶ are presented in Fig. 13, where the dimuon mass spectrum in the vicinity of the J/ψ is shown for O + U and S + U at CERN. For each reaction, central and peripheral collisions are compared by plotting the mass spectrum for high and low E_t events. The two curves are normalized by the continuum, which does not change shape

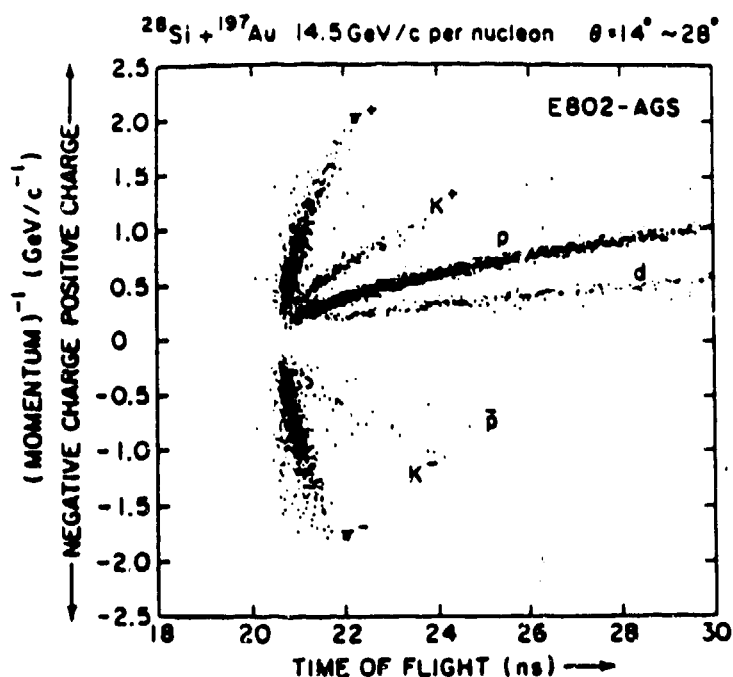


Fig. 12. Scatter plot of TOF vs. $1/p$ for particles observed in the E802 spectrometer for 14.5 GeV/A Si + Au collisions.

with impact parameter, and the area under the J/ψ peaks are compared. It is clear that for both projectiles the high E_t sample contains fewer J/ψ 's in the peak than the low E_t sample. As the continuum does not change, the J/ψ appears to be suppressed for the more central collisions.

This finding has caused great interest as just such a suppression has been predicted as a signal of quark-gluon plasma formation.⁴ It is important, however, to remember that the J/ψ 's are formed early in the collision and are emitted at rather forward angles. They must pass through a large amount of dense matter before reaching the detectors and so there may be absorption effects from the central region or the surrounding spectator matter. Careful study of J/ψ production in p-nucleus collisions is necessary to address this issue and is currently going on both at CERN and at FNAL.²⁷

If the J/ψ suppression is caused by plasma screening a p_t dependent suppression would be expected.²⁸ A high p_t $c\bar{c}$ pair can travel together a large distance from the production point before separating by the J/ψ radius, due to the Lorentz time dilation effect. If p_t is high enough, the pair will traverse

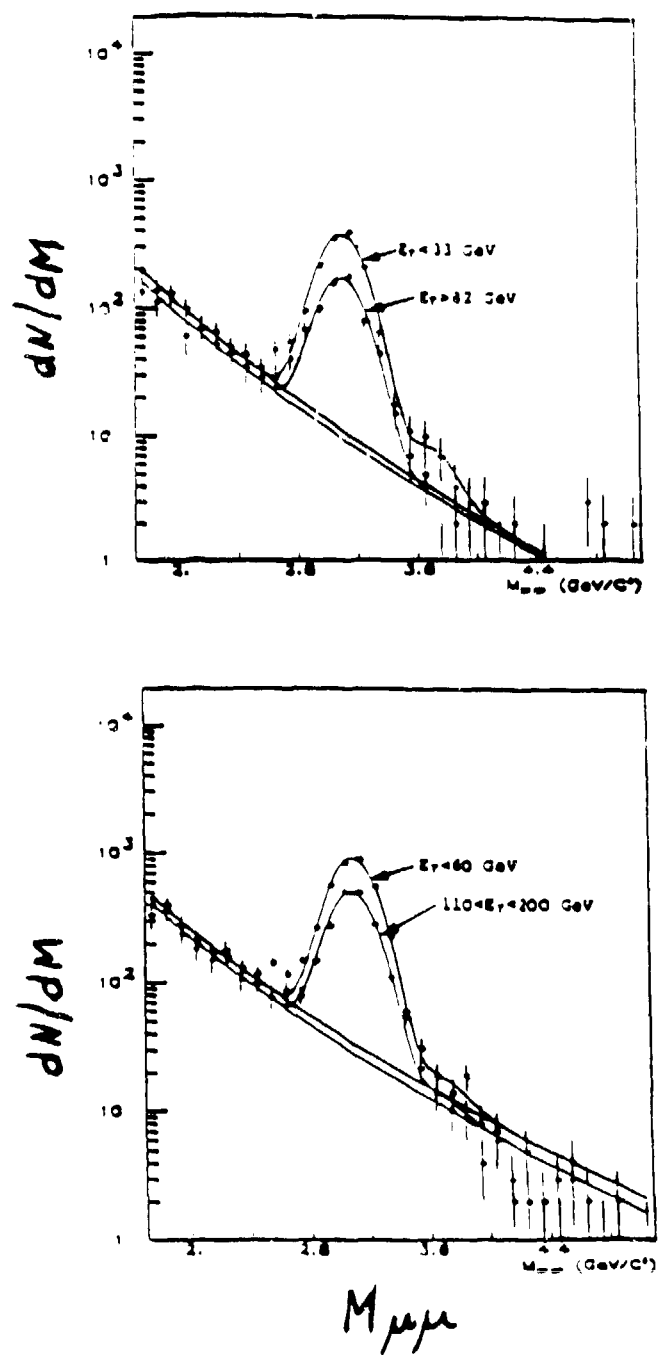


Fig. 13. Dimuon mass spectra measured by NA38 for a) 200 GeV/A O + U and b) 200 GeV/A S + U collisions. The two curves in each part correspond to high and low E_t events. The lines show fits to the J/ψ , ψ' , and continuum.

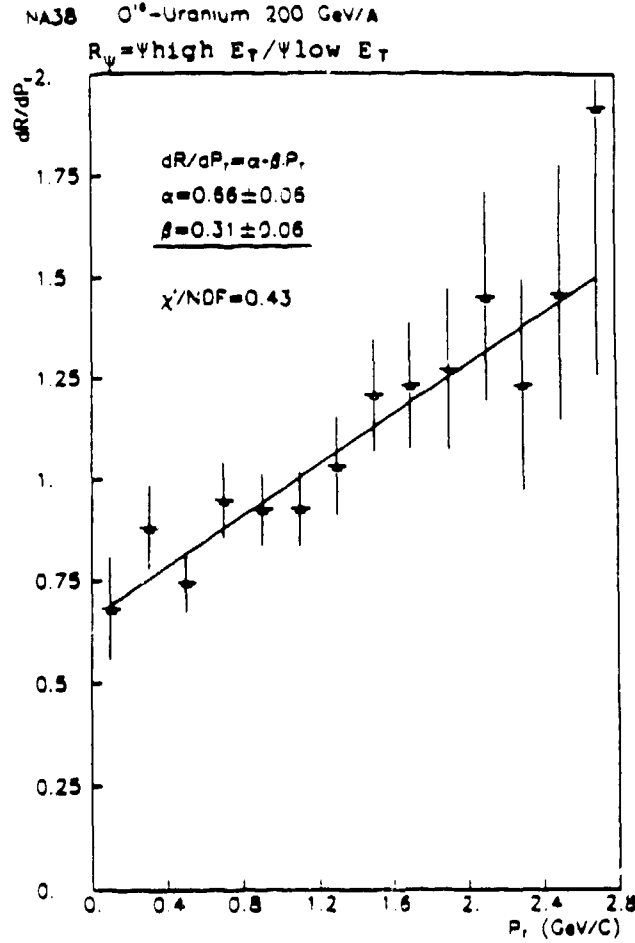


Fig. 14. The ratio of J/ψ for high and low E_T events, as a function of p_t of the dimuon. The data are from NA38 O + U collisions.

the entire transverse dimension of the plasma and come out together, forming a J/ψ . Therefore the suppression should be large at low p_t and disappear for high p_t . To study the p_t dependence of the suppression effect, NA38 has plotted the ratio of observed J/ψ at high and low E_T as a function of p_t . This is shown in Fig. 14 for 200 GeV/A O + U. Clearly, the suppression effect is largest at small p_t . Again, the continuum does not depend on p_t , so the observed effect is a suppression of J/ψ rather than an enhancement of the continuum. It is tempting to draw the conclusion that a plasma is formed, but again absorption effects could be important. These should be larger for low p_t dimuons and simulate the expected effects from plasma screening.

SUMMARY

In summary, we have seen that global variables such as transverse energy and multiplicity can be used to characterize events according to impact parameter. E_t and multiplicity show a linear relationship, indicating that higher E_t arises from production of more particles rather than a large change in the particle spectra. The shapes of the distributions can be explained by superposition of nucleon-nucleon scattering.

There is no large shape difference among the observed charged particle momentum spectra from $p + W$, $O + W$, and $S + W$. We observe no sharp rise in $\langle p_t \rangle$ for large E_t , but it must be noted that the detected p_t spectrum is affected by the hadronization process and reflects conditions at the time of freezeout of hadrons. Also, an increase in the cross section for large p_t is expected from hard scattering of partons and does not necessarily indicate more exotic processes; an increase of approximately this magnitude is observed when comparing peripheral and central collisions.

Two-particle interferometry has been used to determine the size of the source emitting pions. It is found that pion pairs taken over a large rapidity acceptance indicate a rather small source with a radius of ≈ 4 fm, while central rapidity pions indicate a large, nearly spherical source with a high degree of chaoticity and relatively long lifetime.

Study of dimuon production in the J/ψ mass region has shown a suppression of J/ψ with respect to the continuum in high E_t , i.e. central, heavy ion collisions compared to peripheral collisions. The suppression is strongest for low p_t dimuons. This observation has spurred great interest as such a suppression could be a signature of deconfinement, but careful studies are underway to determine how much of the effect can be explained by nuclear absorption.

REFERENCES

1. See, for example, Proc. of the Quark Matter Conferences in Brookhaven (1984), Helsinki (1984) and Asilomar (1986)
2. E.L. Feinberg, *Nuovo Cimento* **34A**, 489 (1976); T. Goldman *et al.*, *Phys. Rev. D* **20**, 619 (1979).
3. M. Kataja, P.V. Ruuskanen, L. McLerran and H. von Gersdorff, *Phys.*

- Rev. D34, 2755 (1986); X. Wang and R. Hwa, Phys. Rev. D35, 3409 (1987).
4. T. Matsui and H. Satz, Phys. Lett. 178B, 416,(1986).
 5. J. Rafelski, Nucl. Phys. A374, 489 (1982). J. Rafelski, Phys. Lett. B190, 167 (1987).
 6. G. Goldhaber *et al.*, Phys. Rev. 120, 300 (1960); G.I. Kopylov, Phys. Lett. B50, 472 (1974).
 7. R. Albrecht *et al.*, Phys. Lett. 202, 596 (1988).
 8. T. Akesson *et al.*, Z. Phys. C38, 383 (1988).
 9. G. Baym, P. Braun-Munzinger and V. Ruuskanen, Phys.Lett. 190B, 29 (1987); A.D. Jackson and H. Boggild, Nucl. Phys. A470, 669 (1987).
 10. G. Baym, G. Friedman and I. Sarcevic, to be published.
 11. P. Braun-Munzinger *et al.*, Z.Phys. C38,45 (1988).
 12. L.P. Remsberg, M.J. Tannenbaum *et al.*, Z. Phys. C38, 35 (1988).
 13. J.D. Bjorken, Phys Rev. D27, 140 (1983).
 14. J.P. Pansart, report DPhPE 86-06, March 1986; and Nucl.Phys A461,521c (1987).
 15. A. Capella and J. Tran Thanh Van, Phys. Lett. 93B, 146 (1980).
 16. L. Van Hove, Phys. Lett. 118B, 138 (1982).
 17. B. Alper *et al.*, Nucl. Phys. B100, 237 (1975).
 18. D. Antreasyan *et al.*, Phys. Rev. D19, 764 (1979).
 19. D.A. Garbutt *et al.*, Phys. Lett. 67B, 355 (1977).
 20. H. Stroebele *et al.*, Z. Phys. C38, 89 (1988).
 21. J.W. Cronin *et al.*, Phys. Rev. D11, 3105 (1975).
 22. F.B. Yano and S.E. Koonin, Phys. Lett B78, 556 (1978).

23. A. Bamberger *et al.*, Phys. Lett. 203B, 320 (1988).
24. B. Andersson *et al.*, Phys. Rep. 97, 31 (1983). B. Andersson *et al.*, Phys. Scr. 34, 451 (1986).
25. Y. Miake *et al.*, Z. Phys. C38, 135 (1988).
26. A. Bussiere *et al.*, Z. Phys. C38, 117 (1988).
27. see, for example, J.C. Peng, this conference.
28. F. Karsch and R. Petronzio, Phys. Lett. B193,105 (1987).